Prehension of an Anthropomorphic Metamorphic Robotic Hand Based on Opposition Space Model

Guowu Wei[1(✉)], Lei Ren[2], and Jian S. Dai[3]

[1] University of Salford, The Crescent, Salford M5 4WT, UK
g.wei@salford.ac.uk
[2] University of Manchester, Manchester M13 9PL, UK
lei.ren@manchester.ac.uk
[3] King's College London, Strand, London WC2R 2LS, UK
jian.dai@kcl.ac.uk

Abstract. This paper presents constrained prehension of an anthropomorphic metamorphic robotic hand based on opposition based model. Structure of the metamorphic hand is briefly introduced and grasp evaluation based on the opposition-space model is presented. Kinematics of the robotic hand is then established leading to the formulation of grasp constraint laying background for investigation of dexterity and manipulability of the metamorphic robotic hand.

Keywords: Metamorphic robotic hand · Anthropomophic hand · Prehension · Kinematics · Grasp constraint

1 Introduction

Since Dr. Engelberger [1] patented the first industrial robot in the early 1960s, there is a tremendous surge of activity in robotics research; and robot hand, as end-effector of robots in operation today has also attracted growing interest since the Berlichingen hand made for a knight in 1509 [2]. However, the modern robotic hand research only started since 1960s when the Belgrade hand was developed. Although most of the industrial applications prefer two or three-fingered grippers with simple design and robust grasp, teleoperation in hazardous or unstructured environments provided much of the impulsion for developing dexterous multifingered robot hands and a number of them have been presented by researchers in the past three decades, including to name but a few, the Stanford/JPL hand [3], the Utah/MIT hand [4], the DLR hand [5] and the UBH3 hand [6].

Most of the early multifingered hands have a common feature of having a rigid palm and base structure. With more functionality requiring for secure grasping and manipulation of various and complex objects, some of the recent anthropomorphic hands such as the Shadow Hand [7] and the DLR/HIT Hand II [8] and the more recently development of two anthropomorphic hands by IIT (Italian Institute of Technology) [9] and the Bionics [10] have used articulated palms of two to three movable sections to increase dexterity and manipulability of the hands.

Y. Huang et al. (Eds.): ICIRA 2017, Part I, LNAI 10462, pp. 71–83, 2017.
DOI: 10.1007/978-3-319-65289-4_7

However, in contrast to a human hand with a foldable and flexible palm, the above robotic hands lack desired versatility, they can neither provide adaptability of hand morphology nor perform the advanced in-hand manipulation.

The introduction of using the metamorphic mechanism as the palm for the metamorphic robotic three-fingered hand [11] marked a turning point and shed light on using the reconfigurable mechanism as a palm of robotic hands to improve their dexterity and manipulability. Metamorphic mechanisms [12] are a class of mechanisms that are capable of altering topological configurations from one to another with a resultant change in the mobility of mechanisms. Originated from artworks, this class of mechanisms can be extracted from origami folds that change topological structure during motion so as to performing multifunction for various tasks. For robot hand involving metamorphic mechanism, it is expected that it can demonstrate more dexterity, versatility and manipulability for grasps of different kind of conditions and environments including the unstructured environment.

Design a robotic hand that is as dexterous as human hand is always a dream of robotic researchers, based on the metamorphic mechanism, several versions metamorphic robotic hands [11,13] have been developed but grasp performance, dexterity and manipulability of these hands demand further investigation. Using the opposition space prehension models proposed by Iberall [15], this paper establishes kinematics of the anthropomorphic metamorphic robotic hand and explicitly formulates the grasp man and grasp constraint laying background for investigation and measurement of dexterity, versatility, adaptability and manipulability of the proposed metamorphic robotic hand.

2 Opposition-Space-Model Based Prehension of the Anthropomorphic Metamorphic Hand

2.1 Mechanical Structure of the Anthropomorphic Metamorphic Robotic Hand

Based on the previous development of the metamorphic three-fingered hand stemming from an origami fold as having been presented in the patent by Dai [11], a dexterous anthropomorphic metamorphic hand is developed by Wei et al. [13] as illustrated in Fig. 1. The hand consists of a reconfigurable palm and five fingers including a four-DOF thumb, and three-DOF index finger, middle finger, ring finger and litter finger. The reconfigurable palm is a spherical five-bar linkage containing five links l_1 to l_5 with the base link l_5 connected to the wrist. Two actuated joints A and E are introduced for adjusting position and orientation of the spherical reconfigurable palm. Joint A is in particular used to change the structure of the reconfigurable palm by rotating the crank link l_1, forming a four-bar linkage at a metamorphic phase. A 3-phalanx thumb of the hand is amounted at link l_2 with joint T providing the fourth degree of freedom,

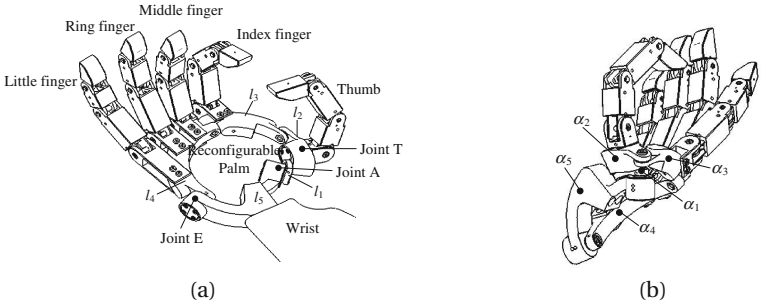

Fig. 1. (a) Mechanical structure of an anthropomorphic metamorphic hand; (b) Metamorphic hand with its palm in a reconfigured position.

a 3-phalanx index finger is mounted at link l_3, and 3-phalanx middle, ring and little fingers are amounted at link l_4. In accordance with the size of an adult's hand, the maximum radius of the spherical linkage palm is assigned as 50 mm. The angles corresponding to links l_1 to l_5 (see Fig. 1b) are α_1 to α_5 complying with $\alpha_1 + \alpha_2 + \alpha_3 + \alpha_4 + \alpha_5 = 2\pi$. In order to increase the dexterity of the palm, both human hand arrangement and rotatability criterion of spherical linkage [14] are considered so that the angles of links are assigned as $\alpha_1 = 25°$, $\alpha_2 = 40°$, $\alpha_3 = 70°$, $\alpha_4 = 112°$ and $\alpha_5 = 113°$. In this case, the fundamental representation of the link angles $\{\bar{\alpha}\}_{i=1}^{5} = \{25°, 40°, 67°, 68°, 70°\}$ satisfies

$$\alpha_1 + \alpha_2 + \alpha_5 = \alpha_3 + \alpha_4. \tag{1}$$

Thus, excluding the indeterminate position where all links fall on a great circle, all joints have full rotatability except for the joint between link 4 and link 5.

2.2 Opposition-Space-Model Based Prehension

Robotic hand is desired to be adaptable to perform specified grasp task and its essential function is prehension. Designed in the above structure, the reconfigurable palm of the robotic hand is foldable, flexible and operated with two degree of freedom. Its operation varies the configuration that subsequently changes the finger base position and finger orientation and subsequently the hand orientation and posture to adapt to different tasks including pinching and twisting. In order to investigate the dexterity of the metamorphic hand, in this section, opposition space model [15] is employed and prehension of the robotic hand is analysed and classified. In the opposition space model, it is proposed that each force applied for grasping is presented by a virtual finger (VF) and each VF is defined as a function unit. Fingers can be grouped into one VF to apply a force or torque opposing to forces or torques applied by other VFs. Once a robotic finger is mapped into a VF, its physical characteristics, i.e., link lengths, joint range of motion and degrees of freedom are mapped into abstract state variables

that describe the VF. In opposition space model, the term opposition is used to describe three basic directions, or primitives, along which the robotic hand can apply force, relative to a hand coordinate frame attached on the palm in Fig. 2. According to the opposition, hand prehension is classified into pad opposition, palm opposition, side opposition, a third virtual finger and the combination of the formers. For each opposition, there exist different virtual finger mappings. For pad opposition, the thumb is used as VF1. For palm opposition, the palm is used as VF1. For side opposition, the thumb is usually used, however, in the adduction grip, the index finger is used. For VF2, one or more fingers can be used.

Pad Opposition. Pad opposition refers to the case that the direction of the opposing forces applied by robotic hand on the specified object parallels to the X-axis. In this case, the robotic hand is expected to exert small forces and impart fine motions to perform the prehensile actions such as pinching a pin, operating scissors and chucking chalk. For the metamorphic hand, these prehensile actions can be realized by change the configuration of the reconfigurable palm and orientation of the thumb as illustrated in Fig. 2. Figure 2c indicates that the size of the palm is reduced when the hand is used to pinch small spherical shaped objects like a small ball and this initially reflects the advantage of this metamorphic hand of a reconfigurable palm.

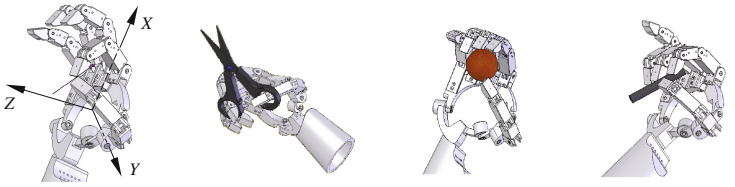

(a) Pinch a pin (b) Operate scissors (c) Pinch a small ball (d) Chuck chalk

Fig. 2. Pad opposition

Palm Opposition. Palm opposition is pertinent to the case that direction of the opposing forces applied by robotic hand on the object is generally perpendicular to the palm (along Z-axis). In this occasion, the robotic hand is expected to match and create larger forces of a stable grasp; this includes grasping big ball and griping sticks. Simulation in Fig. 3 shows that the metamorphic anthropomorphic hand can fulfil these prehensile actions which are realized by driving crank link 1 to adjust the size of the hand, driving link 4 to change orientation of the fingers and driving joint T to further adjust orientation of the thumb. The reconfigurable property of the palm is especially used in Fig. 3d when the hand is used to grasp a stick (for example bar of a hammer) where great force is demanded so that the thumb needs to wrap over the dorsum of the other digits to resist certain forces and couples by providing a powerful buttress on the lateral side.

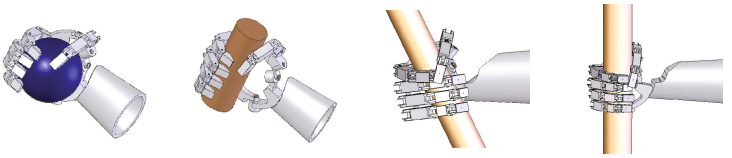

(a) Grasp a big ball (b) Open-fist stick grasp (c) Diagonal volar grasp (d) Closed-fist stick grasp

Fig. 3. Palm opposition

Side Opposition. Side opposition accords with the case that the direction of opposing forces are applied by robotic hand is generally aligned with Y-axis of the hand coordinate frame on the palm. These forces are exerted to the object by putting the thumb pad against the object in opposition to the radial side of a finger in the cases such as pinching a coin or turning a key in Fig. 4b and c, or by putting the radial sides of the index finger and middle finger on both sides of the object to realize the gripping or hold of the small, light object such as a cigarette in Fig. 4a. One can find that although there is no adducted motion between the index finger and the middle finger, this metamorphic hand can fulfil the adduction grip benefiting from the utilizing of the reconfigurable palm which contributes to change the poses of the fingers.

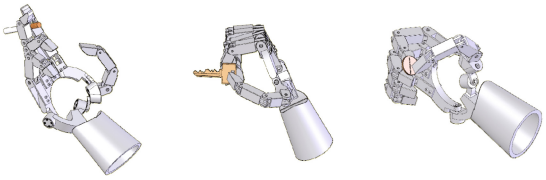

(a) Grip a cigarette (b) Turn a key (c) Pinch a coin

Fig. 4. Side opposition

A Third Virtual Finger and Combination Grasp. A third virtual finger relates to the case of gravity associated grasp in which the hand applies a force against gravity to handle a board or to grasp a hook (see Fig. 5a). This is so-called hook grip where forces from index finger, middle finger, ring finger and little finger need to be exerted on the object continuously for long periods. The metamorphic hand can fulfil this hook grip but the strength of the grip is determined by strength of the tendons which drive the fingers. Further, the versatility of the metamorphic hand, which might not be so much acknowledged, is that it can not only realize any of the aforementioned postures, but also fulfil more complex prehensile actions by combining the above grasping types. In the combined grip, the metamorphic hand can perform the prehensile actions such as holding a cup in Fig. 5b, holding a pencil in Fig. 5c, and simultaneously griping a rod, and pinching a small ball in Fig. 5d.

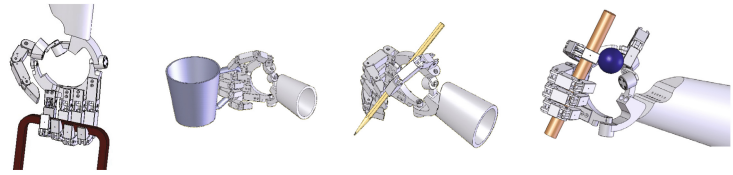

Fig. 5. VF3 and combination grasp

3 Geometry and Kinematics of the Metamorphic Hand

The beneficial effect of the reconfigurable palm can be indicated by its ability of changing palm configuration and changing finger postures to suit various tasks. The motion of l_1 and l_4 results in the change of the palm topological structure. When joint E is fixed at a certain value, the palm operates as a spherical four-bar linkage by evolving into a one-DOF phase. This results in an instant metamorphic phase. When l_2 overlaps the base link l_1, and two links are locked, the palm evolves into a four-bar phase and becomes another one-DOF phase in Fig. 1b. This results in an innate metamorphic phase. While an instant metamorphic phase can always be achieved, the innate metamorphic phase needs to be considered in the mechanical design stage. Thus, with the reconfigurable palm, the metamorphic hand indicates more dexterity, adaptability and manipulability.

In order to reveal the kinematic characteristics of the metamorphic hand, in this section, the geometry and kinematics of the metamorphic hand is investigated based on mechanism decomposition. From mechanism point of view, the metamorphic hand is a hybrid mechanism. Therefore, the whole hand can be decomposed and the kinematics of the metamorphic palm and fingers can be separately studied and then integrated leading to the investigation of the hand kinematics. Closed-form solutions are obtained leading to the prehension and grasping study of the proposed anthropomorphic metamorphic robotic hand.

3.1 Geometric Constraint of the Reconfigurable Palm

Figure 6a gives the schematic diagram of the reconfigurable palm. This is a spherical five-bar linkage with the base link l_5 connected to the wrist. The right-hand-side of the base link connects the first input link l_1 at joint A and the left-hand-side connects the second input link l_4 at joint E. The five fingers are mounted at points F_1 to F_5 respectively. The angle between joint B and OF_1 is δ_1 and angles between joint D and OF_2, OF_3, OF_4, and OF_5 are δ_2, δ_3, δ_4 and δ_5. For various configurations of the palm, points F_1, F_2, F_3, F_4, and F_5 form various pentagons as illustrated in Fig. 6a.

In the spherical five-bar linkage, joints A and E are active joints, and joints B, C and D are passive joints. In order to derive the geometric constraints of this reconfigurable palm, coordinate frames are set up in Fig. 6a in such a way that, for all the local coordinate frames of links l_1 to l_5, they are all centred at

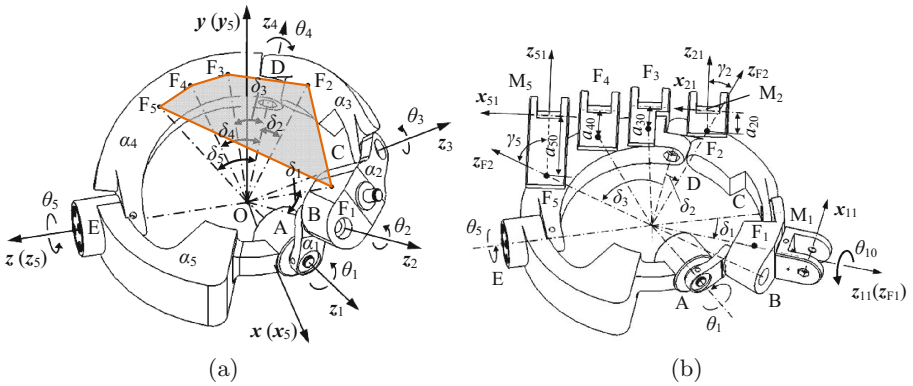

Fig. 6. (a) Parameters of the reconfigurable palm; (b) Parameters of finger base.

point O with z_i-axis aligned with proximal joint of the link l_i, y_i-axis directed along $\boldsymbol{z}_i \times \boldsymbol{z}_{i+1}$ and x_i-axis determined by y_i and z_i with the right-hand rule. A global coordinate frame is set up at point O and has its z-axis aligned with joint E and its y-axis directed along $\boldsymbol{z}_5 \times \boldsymbol{z}_1$, coinciding with y_5 in Fig. 6. Based on this, given the values of angles θ_1 and θ_5, coordinates of points B, C and D can be obtained in the global coordinate frame as

$$\boldsymbol{p}_{\mathrm{B}} = \begin{bmatrix} x_{\mathrm{B}} \\ y_{\mathrm{B}} \\ z_{\mathrm{B}} \end{bmatrix} = \mathbf{R}(y, \alpha_5)\mathbf{R}(z_1, \theta_1)\mathbf{R}(y_1, \alpha_1)\boldsymbol{k} = \begin{bmatrix} c\alpha_1 s\alpha_5 + s\alpha_1 c\alpha_5 c\theta_1 \\ s\alpha_1 s\theta_1 \\ c\alpha_1 c\alpha_5 - s\alpha_1 s\alpha_5 c\theta_1 \end{bmatrix}, \quad (2)$$

$$\begin{aligned} \boldsymbol{p}_{\mathrm{C}} &= \begin{bmatrix} x_{\mathrm{C}} \\ y_{\mathrm{C}} \\ z_{\mathrm{C}} \end{bmatrix} = \mathbf{R}(z_5, \theta_5)\mathbf{R}(y_4, \alpha_4)\mathbf{R}(z_4, \theta_4)\mathbf{R}(y_3, \alpha_3)\boldsymbol{k} \\ &= \begin{bmatrix} c\alpha_3 s\alpha_4 c\theta_5 - s\alpha_3 \left(s\theta_4 s\theta_5 - c\alpha_4 c\theta_4 c\theta_5\right) \\ c\alpha_3 s\alpha_4 s\theta_5 + s\alpha_3 (s\theta_4 s\theta_5 + c\alpha_4 c\theta_4 c\theta_5) \\ c\alpha_3 c\alpha_4 - s\alpha_3 s\alpha_4 c\theta_4 \end{bmatrix} \end{aligned} \quad (3)$$

and

$$\boldsymbol{p}_{\mathrm{D}} = \begin{bmatrix} x_{\mathrm{D}} \\ y_{\mathrm{D}} \\ z_{\mathrm{D}} \end{bmatrix} = \mathbf{R}(z_5, \theta_5)\mathbf{R}(y_4, \alpha_4)\boldsymbol{k} = \begin{bmatrix} c\alpha_4 c\theta_5 \\ s\alpha_4 s\theta_5 \\ c\alpha_4 \end{bmatrix}. \quad (4)$$

Where s and c denote the sine and cosine functions, and $\boldsymbol{k}$ is a unit vector as $\boldsymbol{k} = [0, 0, 1]^{\mathrm{T}}$.

From Fig. 6a, the geometric constraints of the spherical five-bar linkage yield,

$$\boldsymbol{p}_{\mathrm{C}}^{\mathrm{T}} \boldsymbol{p}_{\mathrm{B}} = \cos\alpha_2, \quad (5)$$

$$\boldsymbol{p}_{\mathrm{C}}^{\mathrm{T}} \boldsymbol{p}_{\mathrm{D}} = \cos\alpha_3, \quad (6)$$

$$\boldsymbol{p}_{\mathrm{C}}^{\mathrm{T}}\boldsymbol{p}_{\mathrm{C}} = 1. \tag{7}$$

By solving the about equations, joint angles θ_2, θ_3 and θ_4 can be obtained as

$$\theta_2 = \arctan\frac{F}{E} \pm \arccos\left(\frac{G}{\sqrt{E^2+F^2}}\right) \tag{8}$$

Where, $E = s\alpha_2(s\alpha_1 c\alpha_5 + c\alpha_1 s\alpha_5 c\theta_1)$, $F = -s\alpha_2 s\alpha_5 s\theta_1$ and $G = c\alpha_5(c\alpha_1 c\alpha_5 - s\alpha_1 s\alpha_5 c\theta_1) + (B \mp \sqrt{B^2-4AC})/2A$, with $A = V^2+Q^2+1$, $B = 2(UV+PQ)$ and $C = U^2+P^2-1$, and the terms $U = (y_{\mathrm{D}}c\alpha_2 - y_{\mathrm{B}}c\alpha_3)/(x_{\mathrm{B}}y_{\mathrm{D}} - y_{\mathrm{B}}x_{\mathrm{D}})$, $V = (y_{\mathrm{B}}z_{\mathrm{D}} - z_{\mathrm{B}}y_{\mathrm{D}})/(x_{\mathrm{B}}y_{\mathrm{D}} - y_{\mathrm{B}}x_{\mathrm{D}})$, $P = (x_{\mathrm{B}}c\alpha_3 - x_{\mathrm{D}}c\alpha_2)/(x_{\mathrm{B}}y_{\mathrm{D}} - y_{\mathrm{B}}x_{\mathrm{D}})$ and $Q = (z_{\mathrm{B}}x_{\mathrm{D}} - x_{\mathrm{B}}z_{\mathrm{D}})/(x_{\mathrm{B}}y_{\mathrm{D}} - y_{\mathrm{B}}x_{\mathrm{D}})$.

$$\theta_4 = \arccos(\mathrm{cot}\alpha_3\mathrm{cot}\alpha_4 - z_{\mathrm{C}}/s\alpha_3 s\alpha_4) \tag{9}$$

with $z_{\mathrm{C}} = \frac{-B\pm\sqrt{B^2-4AC}}{2A}$, and

$$\theta_3 = \arctan\frac{F'}{E'} \pm \arccos\left(\frac{G'}{\sqrt{E'^2+F'^2}}\right). \tag{10}$$

Where $E' = s\alpha_3(c\alpha_1 s\alpha_2 + s\alpha_1 c\alpha_2 c\theta_2)$, $F' = -s\alpha_3 s\alpha_1 s\theta_2$ and $G' = c\alpha_3(c\alpha_1 c\alpha_2 - s\alpha_1 s\alpha_2 c\theta_2) - c\alpha_4 c\alpha_5 + s\alpha_4 s\alpha_5 c\theta_5$.

The above gives the motion characteristics of the articulated palm.

3.2 Palm Integrated Whole Hand Kinematics

Fingers of the robotic hand are connected to the above reconfigurable palm through finger bases attached at points F_1, F_2, F_3, F_4 and F_5 as in Fig. 6b. In order to relate palm motion to finger motion, local coordinate frames F_i-$x_{\mathrm{F}i}y_{\mathrm{F}i}z_{\mathrm{F}i}$ are set up at points F_1 to F_5 with $z_{\mathrm{F}i}$-axis directed along OF_i, $y_{\mathrm{F}1}$ directed along $\boldsymbol{z}_{\mathrm{F}1}\times\boldsymbol{z}_3$, $y_{\mathrm{F}2}$ directed along $\boldsymbol{z}_{\mathrm{F}2}\times\boldsymbol{z}_4$, and $y_{\mathrm{F}i}(i=3,4,5)$ directed along $\boldsymbol{z}_{\mathrm{F}i}\times\boldsymbol{z}_5$. Local coordinate frames M_i-$x_{i1}y_{i1}z_{i1}$ $(i=1,2,\ldots,5)$ of the MCP joints of the fingers are set up with x_{i1}-axis aligned with the ith MCP joint and z_{i1}-axis directed along $\mathrm{F}_i\mathrm{M}_i$. The angle between $z_{\mathrm{F}i}$ and z_{i1} is γ_i and the distance between F_i and M_i is a_{i0} as in Fig. 6b. It should be pointed out herein that γ_1 equals 0.

From the above analysis, the coordinate transformations from the finger base coordinate frames to the global coordinate frames can be obtained as

$$\mathbf{R}_{\mathrm{F}i} = \begin{cases} \mathbf{R}(y,\alpha_5)\mathbf{R}(z_1,\theta_1)\mathbf{R}(y_1,\alpha_1)\mathbf{R}(z_2,\theta_2)\mathbf{R}(y_2,\delta_1) & \text{if } i=1 \\ \mathbf{R}(z,\theta_5)\mathbf{R}(y_4,\alpha_4)\mathbf{R}(z_4,\theta_4)\mathbf{R}(y_3,\delta_2) & \text{if } i=2 \\ \mathbf{R}(z,\theta_5)\mathbf{R}(y_4,\alpha_4-\delta_i) & \text{if } i=3,4,5 \end{cases}. \tag{11}$$

Thus, the homogeneous transformation matrix from the finger base coordinate frame to the global coordinate frame can be derived as

$$\mathbf{D}_{\mathrm{F}i} = \begin{bmatrix} \mathbf{R}_{\mathrm{F}i} & \mathbf{R}_{\mathrm{F}i}\boldsymbol{k}' \\ 0 & 1 \end{bmatrix} (i=1,2,\ldots,5), \tag{12}$$

where $\boldsymbol{k} = [0, 0, \mathrm{R}]^{\mathrm{T}}$ and $\mathbf{R}_{\mathrm{F}i}\boldsymbol{k}'$ gives the position vector of point F_i in the global coordinate frame. R is the radius of the sphere on which all the links move.

Then the homogeneous transformation from coordinate frames of the MCP joints to the global coordinate frame can be given according to Fig. 6b as

$$\mathbf{D}_{\mathrm{M}i} = \begin{cases} \mathbf{D}_{\mathrm{F}i}\mathbf{D}_{\mathrm{FM}i}\mathbf{D}_{10} & (\mathrm{i} = 1) \\ \mathbf{D}_{\mathrm{F}i}\mathbf{D}_{\mathrm{FM}i} & (\mathrm{i} = 2, 3, \ldots, 5) \end{cases}, \tag{13}$$

Where, $\mathbf{D}_{\mathrm{FM}i} = \begin{bmatrix} c\gamma_i & 0 & -s\gamma_i & -a_{i0}s\gamma_i \\ 0 & 1 & 0 & 0 \\ s\gamma_i & 0 & c\gamma_i & a_{i0}c\gamma_i \\ 0 & 0 & 0 & 1 \end{bmatrix}$ denotes the transformation from coordinate frame M_i-$x_{i1}y_{i1}z_{i1}$ to coordinate frame F_i-$x_{\mathrm{F}i}y_{\mathrm{F}i}z_{\mathrm{F}i}$. It should be noted that for the thumb finger base, it has γ_1 equals 0. And $\mathbf{D}_{10}$ presents the additional degree of freedom for the thumb as $\mathbf{D}_{10} = \begin{bmatrix} \mathbf{R}(z_{\mathrm{F}1}, \theta_{10}) & 0 \\ 0\ \ 0\ \ 0 & 1 \end{bmatrix}$ with $\mathbf{R}(z_{\mathrm{F}1}, \theta_{10})$ denoting the rotation matrix about $z_{\mathrm{F}1}$ of θ_{10}.

Eventually, given the coordinates of the fingertips in the finger base coordinate frames as $\mathbf{T}_{ft} = e^{[\boldsymbol{s}_{i1}]\theta_{i1}}e^{[\boldsymbol{s}_{i2}]\theta_{i2}}e^{[\mathbf{s}_{i3}]\theta_{i3}}\mathbf{M}$, with $\mathbf{M} = (\mathbf{I}, \boldsymbol{p}_{bt})$ and $\boldsymbol{p}_{bt} = [a_{i1} + a_{i2} + a_{i3}, 0, 0]^T$, where a_{i1}, a_{i2}, and a_{i3} are the lengths of the three phalanxes of the ith finger, the coordinate of the fingertips can be expressed in the global coordinate frame as

$$\mathbf{T}_{f_i} = \mathbf{D}_{M_i}\mathbf{T}_{ft_i}, \tag{14}$$

From Eq. (14), kinematics of the metamorphic hand can be obtained and as shown in [13]. With this kinematic analysis, grasp and prehension of the proposed metamorphic hand presented in Sect. 2.2 can be formulated and investigated.

4 Constraint Representation of Grasp and Prehension

4.1 The Grasp Map and Grasp Constraint

In [16], it is stated that to grasp an object with n fingers contacting it, the grasp map with respect to the object coordinate frame can be given as

$$\mathbf{G} = \left[\mathbf{Ad}^T_{g^{-1}_{oc_1}}\mathbf{B}_{c_1} \quad \cdots \quad \mathbf{Ad}^T_{g^{-1}_{oc_n}}\mathbf{B}_{c_n}\right], \tag{15}$$

with $\mathbf{B}_{ci}$ indicating the wrench basis corresponding to different contact type. And grasp constraint of a multifingered hand grasping have the form

$$\mathbf{J}_h(\theta, x_o)\,\dot{\theta} = \mathbf{G}^T\boldsymbol{V}^b_{po}, \tag{16}$$

where matrix $\mathbf{J}_h(\theta, x_o)$ denotes the hand Jacobian as

$$\mathbf{J}_h(\theta, x_o) = \begin{bmatrix} \mathbf{B}^T_{c_1}\mathbf{Ad}^{-1}_{g_{s_1c_1}}\mathbf{J}^s_{s_1f_1}(\theta_{f_1}) & & 0 \\ & \ddots & \\ 0 & & \mathbf{B}^T_{c_n}\mathbf{Ad}^{-1}_{g_{s_nc_n}}\mathbf{J}^s_{s_nf_n}(\theta_{f_n}) \end{bmatrix},$$

with $\dot{\theta} = (\dot{\theta_{f_1}}, \cdots, \dot{\theta_{f_n}})$ giving the joint velocities, and $\boldsymbol{V}^b_{po}$ is the body velocity of the object expressed in the global coordinate frame.

4.2 Grasp and Prehension Constraint

Considering the opposition-space-model based prehension discussed in Sect. 2.2, and assuming that the contacts type between the fingertips and the objects are of point contact with friction, the grasp and prehension constraints of the metamorphic hand are formulated and presented in this section.

Taking the pinch a small ball in pad opposition indicated in Fig. 2c as an example. Assuming that the thumb, the index finger and the middle finger are involved in this grasp, and the tips of the three fingers are in contact with the ball. Without loss of generality, it is assumed that the contact points between the three fingers and the ball lying on the same plane which passes through the centre of the ball. The object coordinate frame P-$x_o y_o z_o$ is set up at the centre of the ball with its x_o-axis and z_o-axis lie on the same plane which is formed by the three contact points. Contact frames C_i-$x_{c_i} y_{c_i} z_{c_i}$, $i = 1$, 2 and 3 are located at the contact points with z_{c_i}-axis directing towards P and y_{c_i}-axis parallel to y_o-axis. Then, the position of the contact frame with respect to the object frame can be given as

$$\mathbf{R}_{pc_i} = \begin{bmatrix} c\varphi_i & 0 & -s\varphi_i \\ 0 & 1 & 0 \\ s\varphi_i & 0 & c\varphi_i \end{bmatrix} \text{ and } \boldsymbol{p}_{pc_i} = \begin{bmatrix} r_1 s\varphi_i \\ 0 \\ r_1 c\varphi_i \end{bmatrix}. \tag{17}$$

Where φ_i denotes the angle between x_{c_i}-axis and x_o-axis with $i = 1$, 2 and 3, and r_1 is the radius of the ball.

The grasp map for each finger can then be obtained by transforming the standard wrench basis of point contact with friction into the object coordinate frame as

$$\mathbf{G}_i = \begin{bmatrix} \mathbf{R}_{pc_i} & 0 \\ \widehat{\boldsymbol{p}}_{pc_i}\mathbf{R}_{pc_i} & \mathbf{R}_{pc_i} \end{bmatrix} \mathbf{B}_{c_i} = \begin{bmatrix} c\varphi_i & 0 & -s\varphi_i \\ 0 & 1 & 0 \\ s\varphi_i & 0 & c\varphi_i \\ 0 & -r_1 c\varphi_i & 0 \\ r_1 c(2\varphi_i) & 0 & -r_1 s(2\varphi_i) \\ 0 & r_1 s\varphi_i & 0 \end{bmatrix}, \tag{18}$$

where, the wrench basis for each finger is $\mathbf{B}_{c_i} = \begin{bmatrix} \mathbf{I}_{3\times 3} \\ \mathbf{0}_{3\times 3} \end{bmatrix}$, and $i = 1$, 2 and 3.

Substituting Eq. (18) into Eq. (15), the grasp map for the desired prehension can be obtained as $\mathbf{G} = \begin{bmatrix} \mathbf{G}_1 & \mathbf{G}_2 & \mathbf{G}_3 \end{bmatrix}_{6\times 9}$. In the above equations, the parameter φ_i can be determined in the object coordinate frame once the grasp is formed and the contact points are identified. The force-closure property of this grasp can then be detected by convexity conditions.

Further, referring to Fig. 6, each of the fingers is an serial RRR chain, its Jacobian with respect to the finger base coordinate frame has the form

$$\mathbf{J}^{s}_{f_i t_i} = \begin{bmatrix} 0 & a_{i1}s\theta_{i1} & a_{i1}s\theta_{i1} + a_{i2}s(\theta_{i1}+\theta_{i2}) \\ 0 & -a_{i1}c\theta_{i1} & -a_{i1}c\theta_{i1} - a_{i2}c(\theta_{i1}+\theta_{i2}) \\ 0 & 0 & 0 \\ 0 & 0 & 0 \\ 0 & 0 & 0 \\ 1 & 1 & 1 \end{bmatrix}. \tag{19}$$

Where, a_{i1}, a_{i2}, and a_{i3} are the lengths of the three phalanxes of the ith finger, and θ_{i1}, θ_{i2}, and θ_{i3} are the joint angles of the three joints in the ith finger.

According to Eq. (16), in order to formulate the grasp constraint for the grasp of a ball using the metamorphic hand, $\mathbf{Ad}^{-1}_{g_{f_i c_i}}$ needs to be constructed. Based on the geometric relations of coordinate frames established in Fig. 6, there exists

$$\mathbf{Ad}^{-1}_{g_{f_i c_i}} = \mathbf{Ad}^{-1}_{g_{pc_i}} \mathbf{Ad}^{-1}_{g_{op}} \mathbf{Ad}^{-1}_{g_{f_i o}}. \tag{20}$$

In the object coordinate frame, the first term on the right-hand side of Eq. (20) can be written as

$$\mathbf{Ad}^{-1}_{g_{pc_i}} = \begin{bmatrix} \mathbf{R}^T_{pc_i} & -\mathbf{R}^T_{pc_i}\widehat{\boldsymbol{p}}_{pc_i} \\ \mathbf{0} & \mathbf{R}^T_{pc_i} \end{bmatrix}. \tag{21}$$

Substituting Eq. (17) into Eq. (21), it yields

$$\mathbf{Ad}^{-1}_{g_{pc_i}} = \begin{bmatrix} c\varphi_i & 0 & s\varphi_i & 0 & r_1 c(2\varphi_i) & 0 \\ 0 & 1 & 0 & -r_1 c\varphi_i & 0 & r_1 s\varphi_i \\ -s\varphi_i & 0 & c\varphi_i & 0 & -r_1 s(2\varphi_i) & 0 \\ 0 & 0 & 0 & c\varphi_i & 0 & s\varphi_i \\ 0 & 0 & 0 & 0 & 1 & 0 \\ 0 & 0 & 0 & -s\varphi_i & 0 & c\varphi_i \end{bmatrix}. \tag{22}$$

Assume that with respect to the global coordinate frame $O - xyz$ set in the metamorphic hand, the orientation and position of the object coordinate frame, which can be measured through real-time vision system, are given as $\mathbf{R}_{op}$ and $\boldsymbol{p}_{op}$, the second term on the right-hand side of Eq. (20) can be obtained as

$$\mathbf{Ad}^{-1}_{g_{op}} = \begin{bmatrix} \mathbf{R}^T_{op} & -\mathbf{R}^T_{op}\widehat{\boldsymbol{p}}_{op} \\ \mathbf{0} & \mathbf{R}^T_{op} \end{bmatrix}. \tag{23}$$

Finally, substitute terms $\mathbf{R}_{of_i}$ and $\boldsymbol{p}_{of_i}$ in Eq. (14) into the following equation

$$\mathbf{Ad}^{-1}_{g_{f_i o}} = \mathbf{Ad}_{g_{of_i}} = \begin{bmatrix} \mathbf{R}_{of_i} & \widehat{\boldsymbol{p}}_{of_i}\mathbf{R}_{of_i} \\ \mathbf{0} & \mathbf{R}_{of_i} \end{bmatrix}, \tag{24}$$

the third term on the right-hand side of Eq. (20) can be obtained.

Substituting Eqs. (19)–(24) into Eq. (16) gives the hand Jacobian for the pad opposition prehension illustrated in Fig. 2c as

$$\mathbf{J}_h = \begin{bmatrix} \mathbf{J}_{11} & \mathbf{0} & \mathbf{0} \\ \mathbf{0} & \mathbf{J}_{22} & \mathbf{0} \\ \mathbf{0} & \mathbf{0} & \mathbf{J}_{33} \end{bmatrix}_{9\times 9}, \tag{25}$$

where, for $i = 1$, 2 and 3 the 3×3 sub-matrix $\mathbf{J}_{ii}$ is $\mathbf{J}_{ii} = \mathbf{B}_{c_i}^T \mathbf{Ad}_{g_{f_i c_i}}^{-1} \mathbf{J}_{f_i t_i}^s$. This Jacobian matrix can be readily obtained through symbolic computer programme system such as Matlab$^{\text{TM}}$ once all the essential variables are given.

The grasp map and the grasp constraint derived above can be used to evaluate the properties of grasps performed by the metamorphic hand. The grasp map helps to identify whether a grasp performed by the metamorphic hand is force-closure grasp and the grasp constraint helps to determine whether a grasp is manipulable. If for any object motion $\boldsymbol{V}_{op}^b$ there exists $\dot{\theta}$ which satisfies Eq. (16), the grasp executed by the metamorphic hand is supposed to be manipulable.

Using the above formulation, all the prehension cases presented in Sect. 2.2 can be formulated and grasping quality can be measured through the use of convex hull.

5 Conclusions

Prehension of an anthropomorphic metamorphic robotic hand was investigated in this paper based on the principle of opposition space model. Structure of the robotic hand was introduced and grasp evaluation and functionality of the hand was presented using opposition space model. Kinematics of the proposed robotic hand was then established, and grasp map and grasp constraint of the hand were formulated providing explicit mathematical model for representing the opposition space model based prehension. The study presented in this paper hence has laid background for dexterity and manipulability investigation of metamorphic robotic hand and provided insights into grasping measurement for robotic hand development.

References

1. Nof, S.Y.: Handbook of Industrial Robot. Wiley, New York (1985)
2. Childress, D.S.: Artificial hand mechanisms. In: Mechanisms Conference and International Symposium on Gearing and Transmissions (1972)
3. Salisbury, J.K., Craig, J.J.: Articulated hands: force control and kinematic issues. Int. J. Robot. Res. **1**(1), 4–17 (1982)
4. Jacobasen, S.C., Iversen, E.K., Knutti, D.F., Johnson, R.T., Biggers, K.B.: Design of the Utah/M.I.T. dexterous hand. In: IEEE International Conference on Robotics and Automation, pp. 1520–1532 (1986)
5. Tomovic, R., Berkey, G.A., Karplus, W.J.: A strategy for grasp synthesis with multifingered robot hand. In: IEEE International Conference on Robotics and Automation, pp. 83–89 (1987)

6. Lotti, F., Tiezzi, P., Vassura, G.: UBH3: investigating alternative design concepts for robotic hands. In: IEEE International Conference on Robotics Automation, pp. 135–140 (2004)
7. Aminzadeh, V., Walker, R., Cupcic, U., Elias, H., Dai, J.S.: Friction Compensation and Control Strategy for the Dexterous Robotic Hands, Chap. 62, pp. 697–706. Springer, Heidelberg (2013)
8. Liu, H., Wu, K., Meusel, P., Hirzinger, G., Jin, M., Liu, Y., Fan, S., Lan, T., Chen, Z.: A dexterous humanoid five-fingered robotic hand. In: IEEE International Symposium on Robot and Human Interactive Communication, Munich, Germany, pp. 371–376 (2008)
9. NewScientist (2010). http://www.newscientist.com/article/mg20627566.800-robots-with-skin-enter-our-touchyfeely-world.html
10. Fischman, J.: Bionics: National Geographic, pp. 35–53, January 2010
11. Dai, J.S.: Robotic hand with palm section comprising several parts able to move relative to each other (2004). (Patent WO/2005/105391, 10 November 2005; International Patent PCT/GB2005/001665, UK Patent GB04 095 48.5)
12. Dai, J.S., Jones, J.R.: Mobility in metamorphic mechanism of foldable/erectable kinds. ASME Trans. J. Mech. Des. **121**, 375–382 (1999)
13. Wei, G., Dai, J.S., Wang, S., Luo, H.: Kinematic analysis and prototype of a metamorphic anthropomorphic hand with a reconfigurable palm. Int. J. Humanoid Robotics **8**(3), 459–479 (2011)
14. Liu, Y., Ting, K.: On the rotatability of spherical N-bar chains. ASME Trans. J. Mech. Des. **116**(5), 920–923 (1994)
15. Iberall, T.: Human prehension and dexterous robot hands. Int. J. Robot. Res. **16**(3), 285–299 (1997)
16. Murray, R.M., Li, Z., Sastry, S.S.: A Mathematical Introduction to Robotic Manipulation. CRC Press, Boca Raton (1994)